Journal of Materials Chemistry

Cite this: J. Mater. Chem., 2012, 22, 14880

www.rsc.org/materials

PAPER

Non-aggregating solvatochromic bipolar benzo[*f*]quinolines and benzo[*a*]acridines for organic electronics†

Atul Goel,*[a] Vijay Kumar,[a] Salil P. Singh,[a] Ashutosh Sharma,[a] Sattey Prakash,[b] Charan Singh[b] and R. S. Anand[b]

Received 20th February 2012, Accepted 21st May 2012
DOI: 10.1039/c2jm31052j

A novel series of light emitting and thermally stable non-aggregating benzannulated quinolines and acridines were designed and prepared from ketene-*S*,*S*-acetal under mild conditions through C–C bond formation. Photophysical and electrochemical analyses of these bipolar N-heterocyclic compounds revealed intense solvatochromism due to the intramolecular charge-transfer character, exemplary for **9b**, which covered PL ranging from blue (480 nm) to green (501 nm) to yellow (562 nm) to orange (589 nm) using aprotic solvents of varying polarity. Organic light emitting devices with a device configuration of ITO/PEDOT:PSS (40 nm)/NPB (20 nm)/(N-heterocyclic compound) (50 nm)/BCP (7 nm)/LiF (0.7 nm)/Al (200 nm) were successfully prepared. The optoelectronic properties of these compounds were altered by controlled tuning of donor–acceptor and aromatic π-conjugation in benzo[*f*]quinolines and benzo[*a*]acridines, which exhibited a low turn-on voltage with electroluminescence ranging from blue (**6c**: λ_{EL} 455 nm) to green (**8a**: λ_{EL} 496 nm) to yellow (**11**: λ_{EL} 545 nm) to red (**9b**: λ_{EL} 630 nm).

Introduction

Over the past two decades, organic fluorophores have received overwhelming scientific and technological attention due to their tremendous potential as bio-imaging agents,[1] chemosensors,[2] fluorescent probes[3] and as electroluminescent materials for organic electronics, particularly for energy saving and harvesting devices like thin-film transistors,[4] photovoltaic cells,[5] and organic light-emitting devices[6] (OLEDs). Most of the organic fluorophores used for OLEDs are either based on small molecule N-/S-/O-heterocyclic compounds, their metal complexes or polymers containing heterocyclic scaffolds.[7]

After the discovery of 8-hydroxyquinoline aluminium complexes (Alq_3) as efficient emitting/electron transporting materials in OLEDs reported by Tang and VanSlyke,[8] the development of electroluminescent quinoline derivatives and their oligomers has accelerated enormously. Quinolines and poly(quinoline)s have high electron mobilities, good thermal stability, high photoluminescence efficiencies and good film forming properties, which are crucial for their use in OLEDs.[9]

However the self-assembly of quinolines in a well-defined architecture through non-covalent interactions such as *face-to-face* or *edge-to-face* π–π stacking not only leads to bathochromic shifts in photoluminescence but also reduces their quantum efficiencies.[9,10] To inhibit such π–π stacking in the quinoline class of organic compounds, we designed non-planar partially hydrogenated benzo[*f*]quinolines, which have not received much attention for OLED applications (Fig. 1). In order to enhance the hole–electron recombination efficiency, a nice strategy is to equip the molecule with bipolar transporting character such as electron-donating and electron withdrawing moieties to permit the formation of both stable cation and anion radicals.[11] We have recently demonstrated how swapping of the electron donor, acceptor and chromophoric moieties onto an aromatic scaffold plays a crucial role in modulating the optical properties of fluorenes,[12] fluoranthenes[13] and pyrenylarenes,[14] leading to efficient light emitting materials.

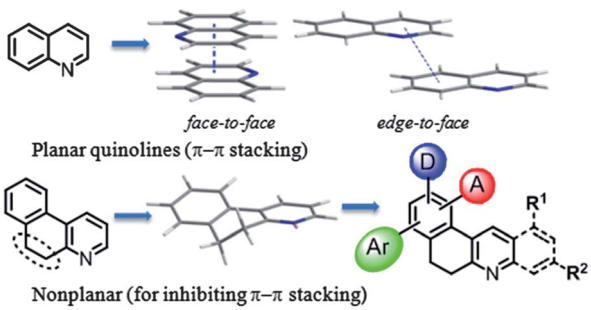

Fig. 1 Design of nonplanar donor–acceptor benzannulated quinolines.

[a]*Division of Medicinal and Process Chemistry, Central Drug Research Institute, CSIR, Lucknow 226001, India. E-mail: atul_goel@cdri.res.in*
[b]*Department of Electrical Engineering, Indian Institute of Technology, Kanpur 208016, India*

† Electronic supplementary information (ESI) available: ^{1}H NMR, ^{13}C NMR and UV, FL, CV graphs of **6a–f**, **8a,b**, **9a,b**, **10**, **11**. See DOI: 10.1039/c2jm31052j

Herein we report the efficient synthesis of non-aggregating bipolar partially hydrogenated benzannulated quinoline derivatives such as benzo[*f*]quinolines and benzo[*a*]acridines, their interesting photophysical and electrochemical properties and their potential use in organic light emitting diodes.

Results and discussion

Synthesis and characterization

Numerous synthetic methodologies are available in the literature for the synthesis of quinoline, acridines and their π-annulated compounds.[15] Recently, a few multicomponent coupling reactions have been employed to furnish benzo[*f*]quinolines in moderate to good yields.[16] We reported a convenient and general methodology for preparing various N-heterocyclic compounds through the base-catalyzed reaction of diverse cyclic or acyclic α,β-unsaturated carbonyl/nitrile compounds with 9-methylacridone.[17] Unfortunately this methodology was unsuccessful for the synthesis of benzo[*a*]acridines due to the unexpectedly high reactivity of the methyl group at position 9 of the acridone. Therefore, we devised a new synthetic route to prepare novel benzo[*f*]quinolines and benzo[*a*]acridines, as shown in Scheme 1.

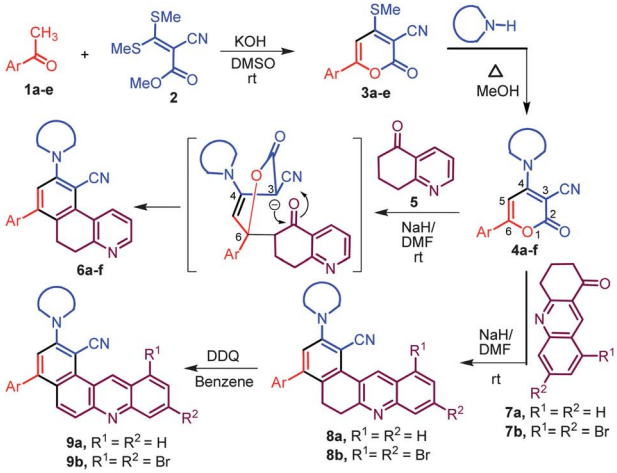

Entry	Amine	Ar	R^1	R^2	Reaction time (min)	Yield (%)
6a	Piperidine	Phenyl	—	—	10	90
6b	Pyrrolidine	Phenyl	—	—	11	88
6c	Piperidine	1-Naphthyl	—	—	12	90
6d	Piperidine	2-Naphthyl	—	—	10	86
6e	Piperidine	Biphenyl	—	—	12	88
6f	Piperidine	1-Pyrenyl	—	—	12	85
8a	Piperidine	Phenyl	H	H	20	82
8b	Piperidine	Phenyl	Br	Br	24	84
9a	Piperidine	Phenyl	H	H	60	70
9b	Piperidine	Phenyl	Br	Br	70	68

Scheme 1 Synthesis of benzo[*f*]quinolines **6a–f** and benzo[*a*]acridines **8a,b** and **9a,b**.

To prepare newly designed molecules with donor–acceptor characteristics, we found a key intermediate α-oxo-ketene-*S*,*S*-acetal with electron acceptor groups suitable for preparing the corresponding lactones **3** following the Tominaga protocol.[18] In order to incorporate a donor functionality such as the *N*,*N*-dialkylamino functionality, a good leaving methylsulfanyl group of lactones **3a–e** was replaced by an amine moiety (piperidine/pyrrolidine) to furnish 6-aryl-2-oxo-4-piperidin/pyrrolidin-1-yl-2*H*-pyran-3-carbonitriles (**4a–f**) in good yields. The reactivity of lactones **4a–f** was explored by the Michael addition of a conjugate base of 7,8-dihydroquinolin-5(6*H*)-one (**5**)[19] or 3,4-dihydroacridin-1(2*H*)-one[20] (**7a,b**) to afford dihydro-benzo[*f*]quinolines or 5,6-dihydro-benzo[*a*]acridines, respectively. Thus, after optimizing the reaction conditions, stirring of an equimolar mixture of **4a–f**, N-heterocyclic ketone **5** or **7a,b** in the presence of NaH in DMF at room temperature furnished bipolar dihydro-benzo[*f*]quinolines **6a–f** or 5,6-dihydro-benzo[*a*]acridines **8a,b**, respectively, in good yields (Scheme 1). For the further tuning of the electronic properties by increasing the conjugation, **8a,b** were treated with DDQ in dry benzene at 80 °C, which afforded fully aromatized substituted benzo[*a*]acridines **9a,b** in good yields (Scheme 1).

In order to inhibit the possible π–π stacking[9a] in planar benzo[*a*]acridines **9**, we incorporated diaryl substituents by exploiting the two C–Br bonds in **8b** using 'Nobel' Suzuki coupling.[21] Thus a mixture of **8b** and phenylboronic acid under basic conditions furnished product **10** in 75% yield (Scheme 2), which was aromatized into 4,9,11-triphenyl-2-(piperidin-1-yl)benzo[*a*]acridine-1-carbonitrile (**11**) in 70% yield using DDQ as an oxidant in dry benzene (Scheme 2).

Optical properties

The photophysical and electrochemical data such as λ_{max} of their UV-vis absorption and photoluminescence (PL) spectra, fluorescence quantum yield, HOMO/LUMO energy levels, and the electrochemical band gap (E_g) of compounds **6a–f**, **8a,b**, **9a,b**, **10** and **11** are shown in Table 1 and Table 2. Fig. 2 shows the normalized UV-vis and PL spectra of selected substances **6a**, **8a,b**, and **9a,b**. The PL maxima of all benzo[*f*]quinolines **6a–f** showed strong blue fluorescence at 455–458 nm with a good fluorescence quantum yield up to 69%. In the case of increasing π-conjugation from benzo[*f*]quinoline **6a** to benzo[*a*]acridines **8a**, a red shift of 12 nm in the PL maxima was observed, while a remarkable red shift of 40 nm was noticed after aromatization of **8a** (PL λ_{max} 468 nm) to **9a** (PL λ_{max} 508 nm). Interestingly

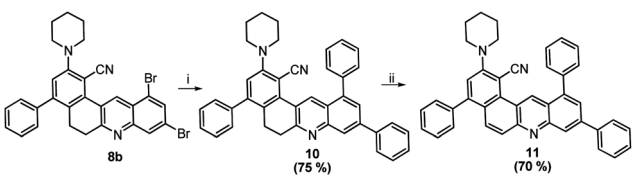

Scheme 2 Synthesis of π-conjugated benzo[*a*]acridines **10** and **11**. *Reaction conditions:* (i) $PdCl_2(PPh_3)_2$, 2M Na_2CO_3, 80 °C, DMF, 45 min.; (ii) DDQ, dry benzene, 80 °C, 1 h.

Table 1 Spectroscopically determined photophysical data of **6a** and **9b** in various solvents

	6a			**9b**		
Solvents (Δf)	$\lambda_{max;abs}$ (nm)	$\lambda_{max;em}$ (nm)	Stoke's shift (cm^{-1})	$\lambda_{max;\ abs}$ (nm)	$\lambda_{max;em}$ (nm)	Stoke's shift (cm^{-1})
Cyclohexane (−0.0014)	360	436	4800	343	480	8300
Toluene (0.0134)	364	448	5200	350	501	8600
THF (0.2096)	360	456	5800	348	540	10000
DMSO (0.2640)	367	471	6000	352	562	10600
DMF (0.2745)	364	468	6100	361	589	10700

dibromo-substituted benzo[*a*]acridines **8b** and **9b** showed PL maxima in the regions of green (**8b**: λ_{max} 508 nm) and yellow (**9b**: λ_{max} 540 nm), respectively, in THF. The replacement of 9,11-dibromo groups in **8b** with 9,11-diphenyl substituents (**10**) showed a hypsochromic shift of about 20 nm, while the aromatization of partially hydrogenated benzo[*a*]acridines **10** to fully aromatized benzo[*a*]acridines **11** exhibited a bathochromic shift of 40 nm due to an increase in π-conjugation.

The solid state fluorescence of the benzo[*f*]quinolines **6a–f** and the benzo[*a*]acridines **8a,b**, **9a,b**, **10**, and **11** were examined in powder form and the data is presented in Table 2. The powder of all benzo[*f*]quinolines **6a–f** showed blue emission characteristics with emission maxima in the range of 456–471 nm. In comparison to the emission spectra of the benzo[*f*]quinolines **6a–f** in dilute solution, the solid state emission data indicates that there is no aggregation in solid state. In order to confirm the non-aggregating behaviour of the synthesized benzoquinolines, we performed classical concentration-dependent photoluminescence analysis of **6c** in THF at different concentrations, as shown in Fig. 3. By increasing the concentration from 10^{-5} M to 10^{-2} M (Fig. 3), the intensity of the PL band increased gradually up to a concentration of 2.5×10^{-4} M and then reduced at 10^{-3} M and 10^{-2} M due to concentration quenching. Importantly, at all concentrations, the emission corresponded only to the monomer at 456 nm (Fig. 3). No red shift or additional peak for excimer formation was observed in benzoquinoline **6c**.

The non-aggregating properties of **6c** were further investigated using a thin film prepared by vacuum evaporation on a glass substrate (see ESI, Fig. S3†). The thin film of **6c** on the glass substrate was continuous and exhibited strong blue emission

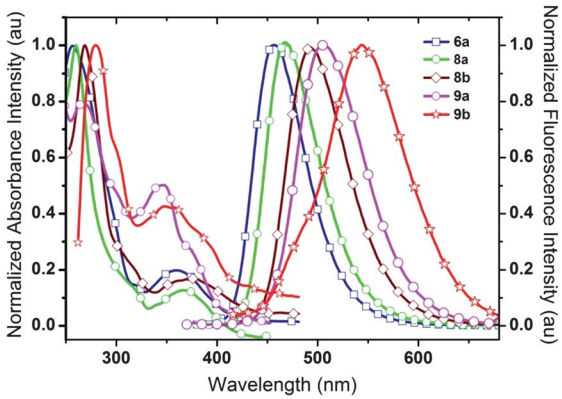

Fig. 2 Normalized absorbance and fluorescence spectra of **6a**, **8a,b** and **9a,b** in THF (~10^{-6} M).

with a maximum at 460 nm, which was only 4 nm red shifted from the emission maxima in dilute solution ($\lambda_{PL,max}$ 456 nm). The solution and solid state PL spectra of **6c** showed that indeed there is no aggregation in solid phase. It is remarkable that all benzo[*f*]quinolines and benzo[*a*]acridines exhibited strong solid-state fluorescence with a wide range of colour emissions due to increasing π-conjugation.

Due to the difference in dipole moments of the donor–acceptor molecules in the ground and excited states and their stabilization by polar or non-polar solvent molecules through various non-covalent interactions like hydrogen bonding, solvation or dipole–dipole interactions, bipolar compounds generally exhibit solvatochromic behaviour. To investigate the stabilization of the

Table 2 Optical and electrochemical properties of **6a–f**, **8a,b**, **9a,b**, **10** and **11**

Entry	$\lambda_{max;abs}$ [a] (nm)	$\lambda_{max;em}$ [b] (nm)	$\lambda_{max;em}$ [c] (nm)	Φ_f [d] (%)	HOMO (eV)	LUMO (eV)	E_g [e] (eV)
6a	257, 360	456	467	63	−5.45	−2.67	2.78
6b	274, 390	455	456	62	−5.28	−2.57	2.71
6c	281, 360	456	468	69	−5.37	−2.65	2.72
6d	257, 362	458	470	60	−5.39	−2.66	2.73
6e	265, 363	457	471	59	−5.38	−2.64	2.74
6f	277, 345	456	471	58	−5.41	−2.67	2.74
8a	260, 367	468	480	46	−5.36	−2.73	2.63
8b	269, 376	490	481	40	−5.40	−2.96	2.44
9a	267, 347	508	525	33	−5.37	−2.96	2.41
9b	279, 348	540	557	31	−5.39	−3.41	1.98
10	268, 369	470	465	51	−5.39	−2.79	2.60
11	283, 348	510	518	37	−5.39	−2.99	2.40

[a] Longest wavelength absorption maximum. [b] PL emission maximum in THF. [c] Fluorescence emission maximum in powder. [d] Fluorescence quantum yield relative to harmine in 0.1 M H_2SO_4 as a standard ($\Phi = 45\%$). [e] Band gap from CV.

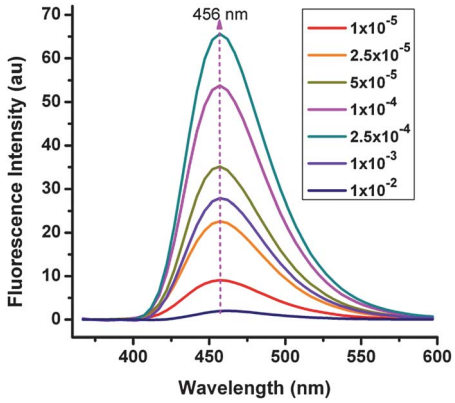

Fig. 3 Fluorescence spectra of **6c** at different concentrations (10^{-5} to 10^{-2} M).

ground and excited states of the synthesized bipolar molecules in various solvents, we examined the absorption and PL spectra of selected N-heterocyclic derivatives **6a** and **9b** using solvents of varying polarity (for **6a** see the ESI†). The benzo[*f*]quinoline **6a** and benzo[*a*]acridine **9b** showed closely resembling absorption profiles upon increasing the polarity of the solvent.

Photoluminescence spectra of the benzo[*f*]quinoline **6a** and benzo[*a*]acridine **9b** were also investigated in a series of solvents with varying polarity index to examine the effect of the polarity of the solvent on the excited state. Interestingly large solvatochromic shifts were observed in the PL emission spectra for the benzo[*f*]quinoline and benzo[*a*]acridine derivatives. For example in the case of **9b** (Fig. 4), the PL maximum increased dramatically with increasing polarity from cyclohexane ($\lambda_{PL,max}$ = 480 nm) to toluene ($\lambda_{PL,max}$ = 501 nm) to THF ($\lambda_{PL,max}$ = 540 nm) to DMSO ($\lambda_{PL,max}$ = 562 nm) to DMF ($\lambda_{PL,max}$ = 589 nm). Further information regarding the solvent sensitivity of the emission spectra of **6a** and **9b** was obtained by evaluation of its Stoke's shift in terms of a Lippert–Mataga plot.[22] Table 1 revealed the changes in emission wavelength and Stoke's shift with increasing solvent polarity.

The correlation of the Stoke's shift ($\Delta\nu$ in cm^{-1}) with the orientation polarizability (Δf) for **6a** and **9b** is represented in Fig. 5. The emission profile of **6a** and **9b** revealed bathochromically shifted emission maxima in the polar solvents such

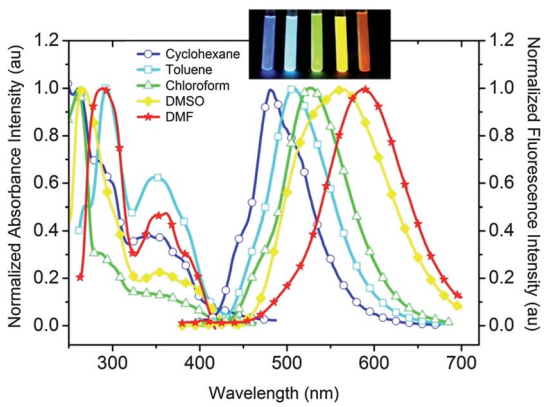

Fig. 4 Solvatochromism shown by **9b** in solvents of varying polarity.

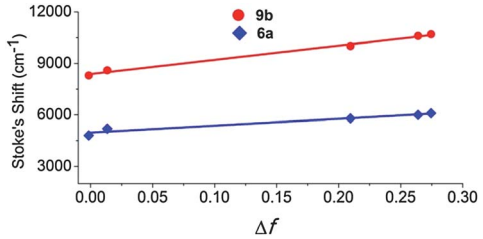

Fig. 5 Lippert–Mataga plot of **6a** and **9b** in solvents of increasing polarity.

as dimethylsulfoxide and dimethylformamide, which exhibited a gradual increase in the Stoke's shift upon increasing the polarity. The slope of the Lippert plot reflects the solvent sensitivity of the fluorophore. For both the dyes, a nice linear correlation (**6a**: r^2 = 0.94, **9b**: r^2 = 0.99) with the orientation polarizability (Δf) was observed (Fig. 5), but the benzo[*a*]acridine dye **9b** exhibited a much steeper slope (8257 cm^{-1}) than benzo[*f*] quinoline **6a** (4017 cm^{-1}), indicating a larger fluorescence solvatochromism for the benzo[*a*]acridine **9b**. The positive solvatochromism indicated that the donor–acceptor benzo[*f*] quinolines and benzo[*a*]acridines exhibited a strongly stabilized excited state with high intramolecular charge transfer (ICT) character and larger dipole moments compared to the ground state by the surrounding solvent molecules.

Electrochemical and thermal properties

Electrochemical studies were carried out to ascertain the redox behavior of the benzo[*f*]quinolines **6a–f** and the benzo[*a*]acridines **8a,b**, **9a,b**, **10** and **11**. All measurements were performed in a three-electrode cell setup using Ag/AgCl as reference electrode and a Pt disc as the working electrode, using a 2 mM solution of compound, and 0.2 M of the electrolyte tetrabutylammonium hexafluorophosphate (Bu_4NPF_6) dissolved in DMF. The cyclic voltammograms obtained were employed to evaluate the highest occupied molecular orbital (HOMO) and the lowest unoccupied molecular orbital (LUMO) energy levels (Fig. 6 and also see ESI†). The HOMO and LUMO levels were readily estimated from the onset oxidation (E_{ox}) and onset reduction potentials (E_{red}), using the equations $E_{HOMO} = -(E_{ox} + 4.8)$ eV and $E_{LUMO} = -(E_{red} + 4.8)$ eV, respectively, where E_{ox} and E_{red} are the onset oxidation and reduction potentials relative to the ferrocene/ferrocenium couple (E_{FOC} = 0.53 V *versus* Ag/AgCl electrode).

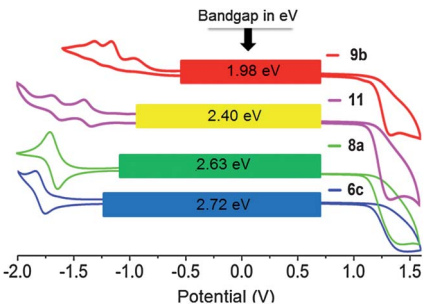

Fig. 6 Cyclic voltammograms of **6c**, **8a**, **9b** and **11** (in DMF).

During the anodic oxidization voltage sweep measured in DMF, irreversible oxidation peaks at 1.47, 1.44, 1.29 and 1.33 V with onset potentials at 1.10, 1.09, 1.12, and 1.12 V for **6c**, **8a**, **11**, and **9b**, respectively, were observed (Fig. 6).

The HOMO energy levels of **6c**, **8a**, **11**, and **9b** were estimated from the oxidation onset potentials, which were found to be −5.37, −5.36, −5.39, and −5.39 eV, respectively (Table 2). The cathodic voltage sweeps for **6c** and **8a** were recorded in DMF, which exhibited reversible reduction waves with half wave potentials ($E_{1/2}$) of −1.79 (E_{pc} = −1.84 V, peak–peak separation ΔE_p = 87 mV) and −1.67 V (E_{pc} = −1.70 V, peak–peak separation ΔE_p = 68 mV), respectively (Fig. 6). Benzo[*a*]acridines **9b** and **11** with longer aromatic π-conjugation showed positively shifted reduction steps (**9b**: three reduction peaks at −0.97, −1.16 and −1.30 V; **11**: two reduction peaks at −1.39 and −1.68 V). Accordingly, the LUMO energy levels of **6c**, **8a**, **11**, and **9b** were calculated from the reduction wave onset potentials to be −2.65, −2.73, −2.99 and −3.41 eV, respectively. Careful examination of the CV graphs revealed that the LUMO levels can be tuned by altering the aromatic π-conjugation without affecting the HOMO levels, as shown in Table 2. The corresponding band gaps of **6c**, **8a**, **11** and **9b** calculated from the HOMO/LUMO values were 2.72, 2.63, 2.40, and 1.98 eV, respectively (Fig. 6).

The thermal properties of **6c**, **8a**, **9b** and **11** were gauged by thermogravimetric analysis (TGA) and differential scanning calorimetry (DSC) (Table 3). **6c**, **8a**, **9b** and **11** are all thermally stable up to 260 °C, as shown by their decomposition temperature (5% weight loss temperature) under nitrogen atmosphere in the TGA measurements. DSC experiments were performed by scanning at a rate of 10 °C min^{-1} under nitrogen atmosphere in the temperature range from 50 to 350 °C. Benzo[*f*]quinoline **6c** and benzo[*a*]acridine **8a** melted at 174 °C and 256 °C respectively, while **11** with a higher molecular weight showed a higher melting temperature of 284 °C.

Electroluminescence properties

Benzo[*f*]quinoline **6c** and benzo[*a*]acridines **8a**, **9b**, and **11** were selected for further electroluminescence studies. Two single-layer OLEDs (Diode 1: ITO/benzo[*f*]quinoline **6c** (100 nm)/LiF (0.7 nm)/Al (200 nm); Diode 2: ITO/PEDOT:PSS (40 nm)/**6c** (100 nm)/LiF (0.7 nm)/Al (200 nm)) were initially fabricated to check the bipolar characteristics of these compounds. The performance of single-layer Diode 1 was not satisfactory while Diode 2 showed a faint blue emission at higher voltage, indicating that the holes and electrons are passing through the device with less recombination. In order to facilitate the recombination efficiency, multilayer devices were fabricated to investigate the performance of multi-colour light-emitting **6c**, **8a**, **9b** and **11** compounds with the device configuration of ITO/PEDOT:PSS (40 nm)/NPB(20 nm)/(N-heterocyclic compound) (50 nm)/BCP (7 nm)/LiF (0.7 nm)/Al (200 nm). The patterned ITO glass plate was cleaned in 6 : 1 : 1 RCA-I solution, rinsed in DI water a number of times and then dried. The ITO surface was treated in ozone for 15 minutes. Immediately, the first layer of poly(3,4-ethylenedioxythiophene) doped with poly(styrenesulfonic acid) (PEDOT:PSS) was spin-coated onto the patterned ITO to form a hole injection layer. The PEDOT:PSS was vacuum dried at 120 °C for 1 hour. All other organic layers and metal layers were sublimed under high vacuum (~1 to 5 × 10^{-6} mbar). A bilayer metal cathode of LiF (0.7 nm)/Al (200 nm) was deposited in a separate vacuum chamber. Then, the devices were sealed with a covering glass plate using UV epoxy. The *ILV* characteristics of the sealed OLED devices were obtained using a Keithley source-measuring unit. EL spectra were recorded with an Ocean Optics USB 2000 fibre optic spectrometer.

The EL characteristics of all four compounds are shown in Fig. 7 and the performance data and Commission Internationale de L'Eclairage (CIE) colour coordinates of the OLEDs **6c**, **8a**, **9b** and **11** are summarized in Table 3. The EL of benzo[*f*]quinoline **6c** showed a sharp peak at 455 nm (blue) with a fwhm of 72 nm, while benzo[*a*]acridines **8a**, **11** and **9b** showed ELs at 496 nm, 545 nm and 630 nm, respectively and an electroluminescence color ranging from blue (CIE 0.18, 0.20) to green (CIE 0.26, 0.43) to yellow (CIE 0.41, 0.53) to red (CIE 0.55, 0.42).

The EL of **6c** exhibited a blue-shift of 4 nm compare to the PL of the thin film of **6c** ($\lambda_{PL,film}$ 460 nm), while similarity with the

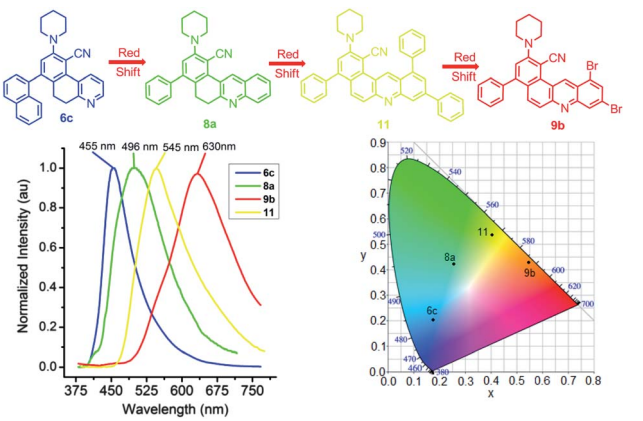

Fig. 7 The EL characteristics and chromaticity diagram showing the CIE coordinates of the OLEDs of **6c**, **8a**, **9b**, and **11**.

Table 3 Thermal stability and performance data of OLEDs of **6c**, **8a**, **9b**, and **11**

Entry	T_d^a/T_m^b (°C)	Turn-on voltage (V)	EL (nm) (λ_{max})	Max. brightness (cd m^{-2})	Max. current eff. (Cd A^{-1})	CIE 1931
6c	260/174	3.5	455	461	0.78	0.18, 0.20
8a	300/256	4	496	39	0.40	0.26, 0.43
11	320/284	6	545	4	0.57	0.41, 0.53
9b	315/260	6	630	0.34	0.0018	0.55, 0.42

[a] Decomposition temperature (5% weight loss) under nitrogen atmosphere in the TGA measurements. [b] Melting temperature gauged by DSC.

photoluminescence of **6c** in THF (λ_{PL} 456 nm) was observed. These results suggested that the EL was attributed to emission from the charge-transfer excited state of benzo[*f*]quinoline **6c** and the partially hydrogenated benzo[*f*]quinoline **6c** did not exhibit aggregation behaviour in device operation. Furthermore, we observed that due to an increase in the planarity by aromatization of the partially hydrogenated benzo[*f*]quinolines to rigid benzo[*a*]acridines, the EL spectra of **8a**, **9b** and **11** showed red-shifts compare to their PL in both solution and solid state. These results supported our design of non-planar partially hydrogenated benzo[*f*]quinolines for OLEDs.

Among the four fabricated multicolour OLEDs, the blue OLED of benzo[*f*]quinoline **6c** showed good stability and performance. The relative energy-level alignments of the fabricated multilayered OLED and the actual device picture of **6c** are shown in Fig. 8.

An unoptimized multilayer OLED of **6c** showed bright blue emission with a low turn-on voltage of 3.5 V and a maximum brightness of 461 cd m^{-2} at 10 V with a current efficiency of 0.78 cd A^{-1}, without using any dopant. Low information content displays like 7-segment and displays for signage and mobile phones have a huge market due to the low operating voltage required to derive these OLED displays with commercially available drivers with 5 V outputs. In order to demonstrate the commercial applications of blue emitter **6c**, a flat panel OLED display using **6c** as emissive material with the device structure ITO/PEDOT:PSS (40 nm)/NPB (20 nm)/**6c** (50 nm)/BCP (7 nm)/LiF (0.7 nm)/Al (200 nm) was fabricated as shown in Fig. 9. The dependence of the device EL on the applied voltage was investigated by increasing the voltage in intervals of 1 V (Fig. 9). The display **6c** showed no change in EL spectrum when the bias was increased up to 12 V, which revealed that the device is electro-optically stable. Further optimization of the device configuration-performance is currently underway.

Experimental

Synthesis of 7-phenyl-9-(piperidin-1-yl)-5,6-dihydrobenzo[*f*]quinoline-10-carbonitrile (6a)

A mixture of 2-oxo-6-phenyl-4-(piperidin-1-yl)-2*H*-pyran-3-carbonitrile (**4a**, 280 mg, 1 mmol), 7,8-dihydroquinolin-5(6*H*)-one (**5**, 176 μL, 1.2 mmol) and NaH (60% dispersion in oil, 60 mg, 1.5 mmol) in dry DMF (5 mL) was stirred at room temperature for 10 min. The progress of reaction was monitored by TLC. On completion, the reaction mixture was poured onto crushed ice with vigorous stirring and finally neutralized with 10% HCl. The precipitate obtained was filtered and purified on a neutral alumina column using 3% ethyl acetate in *n*-hexane as the eluent to afford **6a** (328 mg, 90%) as a light greenish solid: R_f = 0.56 (*n*-hexane–ethyl acetate, 9 : 1, v/v); mp (*n*-hexane–ethyl acetate) 80–82 °C; MS (ESI) 366 [M + H$^+$]; IR (KBr) ν = 3063 (w), 2931 (s), 2820 (m), 2213 (s), 1589 (s) cm^{-1}; ^{1}H NMR (300 MHz, $CDCl_3$): δ = 1.54–1.64 (m, 2H), 1.72–1.86 (m, 4H), 2.68–2.78 (m, 2H), 2.82–2.94 (m, 2H), 3.14–3.26 (m, 4H), 6.94 (s, 1H), 7.27–7.48 (m, 6H), 8.44–8.52 (m, 1H), 8.54–8.62 (m, 1H) ppm; ^{13}C NMR (75 MHz, $CDCl_3$): δ = 23.9, 25.9, 26.1, 32.0, 53.8, 102.6, 118.9, 120.0, 121.7, 127.8, 127.9, 128.4, 128.8, 129.9, 134.5, 138.6, 140.1, 146.1, 148.7, 157.4, 159.2 ppm; HRMS calculated for $C_{25}H_{24}N_3$ [M + H$^+$] 366.1970, found: 366.1968.

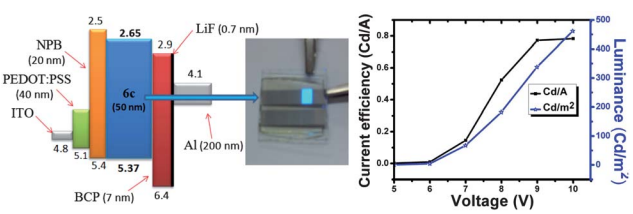

Fig. 8 Relative energy-level alignment and layer thickness, actual device picture, and OLED characteristics of **6c**.

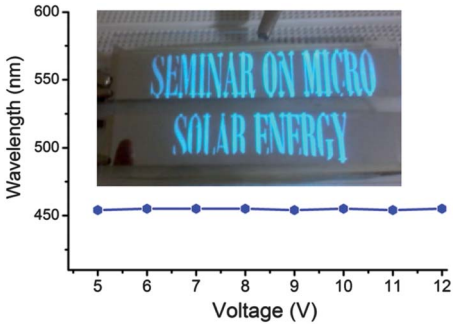

Fig. 9 EL *vs.* voltage graph of **6c** and blue OLED display of donor–acceptor benzo[*f*]quinoline **6c**.

Synthesis of 7-phenyl-9-(pyrrolidin-1-yl)-5,6-dihydrobenzo[*f*]quinoline-10-carbonitrile (6b)

A mixture of 2-oxo-6-phenyl-4-(pyrrolidin-1-yl)-2*H*-pyran-3-carbonitrile (**4b**, 266 mg, 1 mmol), 7,8-dihydroquinolin-5(6*H*)-one (**5**, 176 μL, 1.2 mmol) and NaH (60% dispersion in oil, 60 mg, 1.5 mmol) in dry DMF (5 mL) was stirred at room temperature for 11 min. The progress of reaction was monitored by TLC and on completion, the reaction mixture was poured onto crushed ice with vigorous stirring and finally neutralized with 10% HCl. The precipitate obtained was filtered and purified on a neutral alumina column using 3% ethyl acetate in *n*-hexane as the eluent to afford **6b** (309 mg, 88%) as a light greenish solid: R_f = 0.54 (*n*-hexane–ethyl acetate, 9 : 1, v/v); mp (*n*-hexane–ethyl acetate) 146–148 °C; MS (ESI) 352 [M + H$^+$]; IR (KBr) ν = 3037 (m), 2931 (s), 2856 (w), 2806 (s), 2214 (s), 1597 (s), 1488 (s) cm^{-1}; ^{1}H NMR (300 MHz, $CDCl_3$): δ = 1.96–2.08 (m, 4H), 2.62–2.74 (m, 2H), 2.82–2.96 (m, 2H), 3.52–3.70 (m, 4H), 6.68 (s, 1H), 7.27–7.50 (m, 6H), 8.42–8.54 (m, 2H) ppm; ^{13}C NMR (50 MHz, $CDCl_3$): δ = 25.6, 25.9, 32.3, 50.9, 91.7, 115.4, 120.8, 121.5, 125.5, 127.8, 128.1, 128.3, 128.7, 135.0, 139.0, 140.6, 146.1, 148.5, 152.1, 159.5 ppm; HRMS calculated for $C_{24}H_{22}N_3$ [M + H$^+$] 352.1813, found: 352.1801.

Synthesis of 7-(naphthalen-1-yl)-9-(piperidin-1-yl)-5,6-dihydrobenzo[*f*]quinoline-10-carbonitrile (6c)

A mixture of 6-(naphthalen-1-yl)-2-oxo-4-(piperidin-1-yl)-2*H*-pyran-3-carbonitrile (**4c**, 330 mg, 1 mmol), 7,8-dihydroquinolin-5(6*H*)-one (**5**, 176 μL, 1.2 mmol) and NaH (60% dispersion in oil, 60 mg, 1.5 mmol) in dry DMF (5 mL) was stirred at room temperature for 12 min. The progress of reaction was monitored

by TLC and on completion, the reaction mixture was poured onto crushed ice with vigorous stirring and finally neutralized with 10% HCl. The precipitate obtained was filtered and purified on a neutral alumina column using 3% ethyl acetate in *n*-hexane as the eluent to afford **6c** (374 mg, 90%) as a light greenish solid: $R_f = 0.52$ (*n*-hexane–ethyl acetate, 9 : 1, v/v); mp (*n*-hexane–ethyl acetate) 172–174 °C; MS (ESI) 416 [M + H$^+$]; IR (KBr) $\nu = 3050$ (w), 2930 (s), 2849 (m), 2208 (s), 1586 (s) cm^{-1}; ^{1}H NMR (300 MHz, $CDCl_3$): $\delta = 1.54$–1.66 (m, 2H), 1.74–1.88 (m, 4H), 2.34–2.48 (m, 2H), 2.76–2.82 (m, 2H), 3.12–3.28 (m, 4H), 6.98 (s, 1H), 7.28–7.58 (m, 6H), 7.84–7.98 (m, 2H), 8.42–8.52 (m, 1H), 8.58–8.72 (m, 1H) ppm; ^{13}C NMR (75 MHz, $CDCl_3$): $\delta = 24.0$, 25.7, 26.2, 32.0, 54.0, 102.8, 119.1, 120.8, 121.9, 125.3, 125.4, 126.2, 126.5, 126.7, 127.9, 128.4, 128.5, 131.4, 133.5, 134.6, 138.0, 138.3, 144.6, 148.9, 157.6, 159.4 ppm; HRMS calculated for $C_{29}H_{26}N_3$ [M$^+$ + H] 416.2126, found: 416.2118.

Synthesis of 7-(naphthalen-2-yl)-9-(piperidin-1-yl)-5,6-dihydrobenzo[*f*]quinoline-10-carbonitrile (6d)

A mixture of 6-(naphthalen-2-yl)-2-oxo-4-(piperidin-1-yl)-2*H*-pyran-3-carbonitrile (**4d**, 330 mg, 1 mmol), 7,8-dihydroquinolin-5(6*H*)-one (**5**, 176 μL, 1.2 mmol) and NaH (60% dispersion in oil, 60 mg, 1.5 mmol) in dry DMF (6 mL) was stirred at room temperature for 10 min. The progress of reaction was monitored by TLC and on completion, the reaction mixture was poured onto crushed ice with vigorous stirring and finally neutralized with 10% HCl. The precipitate obtained was filtered and purified on a neutral alumina column using 3% ethyl acetate in *n*-hexane as the eluent to afford **6d** (357 mg, 86%) as a light greenish solid: $R_f = 0.53$ (*n*-hexane–ethyl acetate, 9 : 1, v/v); mp (*n*-hexane–ethyl acetate) 132–134 °C; MS (ESI) 416 [M + H$^+$]; IR (KBr) $\nu = 3032$ (w), 2930 (s), 2820 (m), 2213 (s), 1587 (s) cm^{-1}; ^{1}H NMR (300 MHz, $CDCl_3$): $\delta = 1.54$–1.64 (m, 2H), 1.74–1.88 (m, 4H), 2.68–2.92 (m, 4H), 3.12–3.28 (m, 4H), 7.04 (s, 1H), 7.28–7.56 (m, 4H), 7.76–7.98 (m, 4H), 8.46–8.54 (m, 1H), 8.60 (d, $J = 7.9$ Hz, 1H) ppm; ^{13}C NMR (75 MHz, $CDCl_3$): $\delta = 23.9$, 26.0, 26.1, 31.9, 53.9, 102.6, 119.0, 120.2, 121.8, 126.5, 126.6, 126.7, 127.7, 127.8, 127.9, 128.0, 130.1, 132.6, 133.0, 134.6, 137.6, 138.6, 146.1, 148.7, 157.5, 159.2 ppm; HRMS calculated for $C_{29}H_{26}N_3$ [M$^+$ + H] 416.2126, found: 416.2135.

Synthesis of 7-(biphenyl-4-yl)-9-(piperidin-1-yl)-5,6-dihydrobenzo[*f*]quinoline-10-carbonitrile (6e)

A mixture of 6-(biphenyl-4-yl)-2-oxo-4-(piperidin-1-yl)-2*H*-pyran-3-carbonitrile (**4e**, 356 mg, 1 mmol), 7,8-dihydroquinolin-5(6*H*)-one (**5**, 176 μL, 1.2 mmol) and NaH (60% dispersion in oil, 60 mg, 1.5 mmol) in dry DMF (6 mL) was stirred at room temperature for 12 min. The progress of reaction was monitored by TLC and on completion, the reaction mixture was poured onto crushed ice with vigorous stirring and finally neutralized with 10% HCl. The precipitate obtained was filtered and purified on a neutral alumina column using 3% ethyl acetate in *n*-hexane as the eluent to afford **6e** (388 mg, 88%) as a light greenish solid: $R_f = 0.50$ (*n*-hexane–ethyl acetate, 9 : 1, v/v); mp (*n*-hexane–ethyl acetate) 152–154 °C; MS (ESI) 442 [M + H$^+$]; IR (KBr) $\nu = 3019$ (w), 2939 (s), 2851 (w), 2851 (w), 2215 (s), 1589 (s) cm^{-1}; ^{1}H NMR (300 MHz, $CDCl_3$): $\delta = 1.54$–1.68 (m, 2H), 1.76–1.92 (m, 4H), 2.76–2.98 (m, 4H), 3.12–3.28 (m, 4H), 6.99 (s, 1H), 7.30–7.54 (m, 6H), 7.58–7.76 (m, 4H), 8.44–8.54 (m, 1H), 8.59 (d, $J = 6.9$ Hz, 1H) ppm; ^{13}C NMR (75 MHz, $CDCl_3$): $\delta = 24.0$, 26.0, 26.1, 32.0, 53.9, 102.6, 118.9, 120.2, 121.8, 127.0, 127.1, 127.6, 127.8, 128.8, 129.3, 130.0, 134.5, 138.7, 139.0, 140.3, 140.9, 145.7, 148.8, 157.5, 159.3 ppm; HRMS calculated for $C_{31}H_{28}N_3$ [M$^+$ + H] 442.2283, found: 442.2257.

Synthesis of 9-(piperidin-1-yl)-7-(pyren-1-yl)-5,6-dihydrobenzo[*f*]quinoline-10-carbonitrile (6f)

A mixture of 2-oxo-4-(piperidin-1-yl)-6-(pyren-1-yl)-2H-pyran-3-carbonitrile (**4f**, 404 mg, 1 mmol), 7,8-dihydroquinolin-5(6*H*)-one (**5**, 176 μL, 1.2 mmol) and NaH (60% dispersion in oil, 60 mg, 1.5 mmol) in dry DMF (5 mL) was stirred at room temperature for 12 min. The progress of reaction was monitored by TLC and on completion, the reaction mixture was poured onto crushed ice with vigorous stirring and finally neutralized with 10% HCl. The precipitate obtained was filtered and purified on a neutral alumina column using 3% ethyl acetate in *n*-hexane as the eluent to afford **6f** (416 mg, 85%) as a light greenish solid: $R_f = 0.54$ (*n*-hexane–ethyl acetate, 9 : 1, v/v); mp (*n*-hexane–ethyl acetate) 214–216 °C; MS (ESI) 490 [M + H$^+$]; IR (KBr) $\nu = 2934$ (s), 2851 (w), 2212 (s), 1588 (s) cm^{-1}; ^{1}H NMR (300 MHz, $CDCl_3$): $\delta = 1.54$–1.68 (m, 2H), 1.74–1.88 (m, 4H), 2.38–2.46 (m, 2H), 2.78–2.88 (m, 2H), 3.14–3.28 (m, 4H), 7.10 (s, 1H), 7.32–7.38 (m, 1H), 7.73 (d, $J = 9.1$ Hz, 1H), 7.88 (d, $J = 7.8$ Hz, 1H), 7.97–8.32 (m, 7H), 8.46–8.54 (m, 1H), 8.69 (d, $J = 7.8$ Hz, 1H) ppm; ^{13}C NMR (75 MHz, $CDCl_3$): $\delta = 24.0$, 25.8, 26.2, 31.9, 53.9, 102.8, 119.1, 121.1, 121.8, 124.5, 124.6, 124.6, 125.3, 125.6, 126.3, 126.7, 127.2, 127.9, 128.2, 128.7, 130.8, 131.1, 131.3, 131.5, 134.6, 135.1, 138.4, 145.0, 148.9, 157.5, 159.4 ppm; HRMS calculated for $C_{35}H_{28}N_3$ [M$^+$ + H] 490.2283, found: 490.2213.

Synthesis of 4-phenyl-2-(piperidin-1-yl)-5,6-dihydrobenzo[*a*]acridine-1-carbonitrile (8a)

A mixture of 2-oxo-6-phenyl-4-(piperidin-1-yl)-2*H*-pyran-3-carbonitrile (**4a**, 280 mg, 1 mmol), 3,4-dihydroacridin-1(2*H*)-one (**7a**, 197 mg, 1 mmol) and NaH (60% dispersion in oil, 60 mg, 1.5 mmol, 1.5 equiv.) in dry DMF (10 mL) was stirred at room temperature for 20 min. The progress of reaction was monitored by TLC, and upon completion, the solvent was evaporated and the reaction mixture was poured onto crushed ice with vigorous stirring and finally neutralized with 10% HCl. The precipitate obtained was filtered and purified on a silica gel column using 20% ethyl acetate in *n*-hexane as the eluent to afford 340 mg (82%) of **8a** as a light yellow solid: $R_f = 0.52$ (ethyl acetate–*n*-hexane, 1 : 9, v/v); mp (ethyl acetate–*n*-hexane) 254–256 °C; MS (ESI) 416 [M + H$^+$]; IR (KBr) $\nu = 2937$ (s), 2851 (m), 2207 (s), 1581 (s) cm^{-1}; ^{1}H NMR (300 MHz, $CDCl_3$): $\delta = 1.56$–1.68 (m, 2H), 1.78–1.95 (m, 4H), 2.78–2.90 (m, 2H), 3.01–3.14 (m, 2H), 3.21–3.30 (m, 4H), 6.97 (s, 1H), 7.28–7.60 (m, 6H), 7.68–7.78 (m, 1H), 7.95 (d, $J = 7.9$ Hz, 1H) 8.03 (d, $J = 8.5$ Hz, 1H), 9.02 (s, 1H); ^{13}C NMR (75 MHz, $CDCl_3$): $\delta = 24.1$, 26.1, 26.3, 33.3, 54.1, 102.9, 119.3, 120.3, 124.8, 125.9, 126.3, 127.3, 128.0, 128.2, 128.5, 128.6, 128.9, 130.4, 130.5, 134.6, 138.8, 140.2, 146.2, 147.2, 157.7, 160.4 ppm; HRMS calculated for $C_{29}H_{26}N_3$ [M$^+$ + H] 416.2127, found: 416.2126.

Synthesis of 9,11-dibromo-4-phenyl-2-(piperidin-1-yl)-5,6-dihydrobenzo[*a*]acridine-1-carbonitrile (8b)

A mixture of 2-oxo-6-phenyl-4-(piperidin-1-yl)-2*H*-pyran-3-carbonitrile (**4a**, 280 mg, 1 mmol), 6,8-dibromo-3,4-dihydroacridin-1(2*H*)-one (**7b**, 355 mg, 1 mmol) and NaH (60% dispersion in oil, 60 mg, 1.5 mmol) in dry DMF (8 mL) was stirred at room temperature for 24 min. The progress of reaction was monitored by TLC and on completion, the solvent was evaporated and the reaction mixture was poured onto crushed ice with vigorous stirring and finally neutralized with 10% HCl. The precipitate obtained was filtered and purified on a silica gel column using 20% ethyl acetate in *n*-hexane as the eluent to afford 580 mg (84%) of **8b** as a light yellow solid: $R_f = 0.72$ (ethyl acetate–*n*-hexane, 1 : 9, v/v); mp (ethyl acetate–*n*-hexane) 244–246 °C; MS (ESI) 572 [M + H$^+$]; IR (KBr) $\nu = 2920$ (s), 2805 (w), 2205 (s), 1584 (w) cm^{-1}; ^{1}H NMR (300 MHz, $CDCl_3$): $\delta = 1.58$–1.68 (m, 2H), 1.79–1.90 (m, 4H), 2.78–2.90 (m, 2H), 3.10–3.30 (m, 6H), 7.00 (s, 1H), 7.30–7.38 (m, 2H), 7.40–7.51 (m, 3H), 8.02–8.16 (m, 2H), 8.89 (s, 1H); ^{13}C NMR (75 MHz, $CDCl_3$): $\delta = 24.0$, 26.0, 26.2, 33.4, 53.9, 102.9, 119.0, 119.3, 120.8, 124.8, 127.6, 128.2, 128.6, 128.9, 129.2, 130.3, 130.7, 133.6, 136.2, 137.7, 139.9, 143.0, 146.5, 157.8, 161.7 ppm; HRMS calculated for $C_{29}H_{24}Br_2N_3$ [M$^+$ + H] 572.0337, found: 572.0337.

Synthesis of 4-phenyl-2-(piperidin-1-yl)benzo[*a*]acridine-1-carbonitrile (9a)

4-Phenyl-2-(piperidin-1-yl)-5,6-dihydrobenzo[*a*]acridine-1-carbonitrile (**8a**, 415 mg, 1 mmol) was treated with DDQ (554 mg, 2 mmol) in refluxing benzene for 60 min. After completion, the reaction mixture was filtered and the filtrate was evaporated under reduced pressure. The crude product obtained was purified by column chromatography on neutral alumina using 10% ethyl acetate in *n*-hexane as the eluent to afford 289 mg (70%) of **9a** as a yellow solid: $R_f = 0.58$ (ethyl acetate–*n*-hexane, 1 : 9, v/v); mp (ethyl acetate–*n*-hexane) 240–242 °C; MS (ESI) 414 [M + H$^+$]; IR (KBr) $\nu = 2929$ (s), 2839 (m), 2206 (s), 1563 (m) cm^{-1}; ^{1}H NMR (300 MHz, $CDCl_3$): $\delta = 1.65$–1.76 (m, 2H), 1.82–1.97 (m, 4H), 3.40–3.52 (m, 4H), 7.30 (s, 1H), 7.42–7.70 (m, 6H), 7.82–7.92 (m, 3H), 8.18–8.28 (m, 2H), 10.66 (s, 1H); ^{13}C NMR (75 MHz, $CDCl_3$): $\delta = 24.1$, 26.2, 54.1, 99.2, 120.4, 121.1, 122.6, 124.4, 125.9, 126.1, 127.4, 128.3, 128.5, 128.6, 129.2, 129.4, 129.8, 131.2, 133.5, 134.8, 139.8, 146.9, 148.4, 149.5, 159.3 ppm; HRMS calculated for $C_{29}H_{24}N_3$ [M$^+$ + H] 414.1970, found: 414.1977.

Synthesis of 9,11-dibromo-4-phenyl-2-(piperidin-1-yl)benzo[*a*]acridine-1-carbonitrile (9b)

9,11-Dibromo-4-phenyl-2-(piperidin-1-yl)-5,6-dihydrobenzo[*a*]acridine-1-carbonitrile (**8b**, 571 mg, 1 mmol) was treated with DDQ (554 mg, 2 mmol) in refluxing benzene for 70 min. After completion, the reaction mixture was filtered and the filtrate was evaporated under reduced pressure. The crude product obtained was purified by column chromatography on neutral alumina using 10% ethyl acetate in *n*-hexane as the eluent to afford 387 mg (68%) of **9b** as a red solid: $R_f = 0.76$ (ethyl acetate–*n*-hexane, 1 : 9, v/v); mp (ethyl acetate–*n*-hexane) 256–258 °C; MS (ESI) 570 [M + H$^+$]; IR (KBr) $\nu = 2930$ (s), 2813 (m), 2214 (s), 1572 (w) cm^{-1}; ^{1}H NMR (300 MHz, $CDCl_3$): $\delta = 1.65$–1.75 (m, 2H), 1.85–1.98 (m, 4H), 3.40–3.52 (m, 4H), 7.32 (s, 1H), 7.43–7.60 (m, 5H), 7.88–7.96 (m, 2H), 8.25–8.38 (m, 2H), 10.54 (s, 1H); ^{13}C NMR (75 MHz, $CDCl_3$): $\delta = 24.1$, 26.2, 54.1, 99.3, 118.9, 120.9, 121.1, 123.6, 124.8, 125.1, 127.1, 127.5, 128.5, 128.7, 129.8, 130.3, 130.8, 132.8, 134.3, 137.0, 139.5, 143.8, 147.1, 150.3, 159.4 ppm; HRMS calculated for $C_{29}H_{22}Br_2N_3$ [M$^+$ + H] 570.0180, found: 570.0178.

Synthesis of 2-(piperidin-1-yl)-4,9,11-triphenyl-5,6-dihydrobenzo[*a*]acridine-1-carbonitrile (10)

The solution of 9,11-dibromo-4-phenyl-2-(piperidin-1-yl)-5,6-dihydrobenzo[*a*]acridine-1-carbonitrile (**8b**, 569 mg, 1 mmol) and phenylboronic acid (268 mg, 2.2 mmol) in DMF (8 mL) was degassed with nitrogen for 20 min followed by addition of Na_2CO_3 (3.0 mL, 2 M) under continuous flow of nitrogen. $PdCl_2(PPh_3)_2$ (280 mg, 0.40 mmol) was added to the reaction mixture under a nitrogen atmosphere. The reaction mixture was stirred at 80 °C for 45 min. After completion, the reaction mixture was diluted with H_2O (5 mL), and then extracted four times with ethyl acetate (10 mL). The combined organic layer was dried over Na_2SO_4 and the solvent was removed *in vacuo*. The crude product was purified on a silica gel column using hexane : ethyl acetate (8 : 2, v/v) as eluent to afford 426 mg (75%) of **10** as a yellow solid; $R_f = 0.74$ (ethyl acetate–*n*-hexane, 1 : 9, v/v); mp (ethyl acetate–*n*-hexane) > 250 °C; MS (ESI) 568 [M + H$^+$]; IR (KBr) $\nu = 2929$ (s), 2854 (w), 2215 (s), 1458 (w) cm^{-1}; ^{1}H NMR (300 MHz, $CDCl_3$): $\delta = 1.60$–1.70 (m, 2H), 1.78–1.90 (m, 4H), 2.74–2.84 (m, 2H), 2.98–3.05 (m, 2H), 3.20–3.32 (m, 4H), 6.97 (s, 1H), 7.32–7.60 (m, 11H), 7.75–7.88 (m, 4H), 8.02–8.06 (m, 1H), 8.13–8.16 (m, 1H), 9.09 (s, 1H); ^{13}C NMR (75 MHz, $CDCl_3$): $\delta = 24.1$, 26.2, 26.3, 33.4, 54.0, 102.9, 119.4, 120.1, 125.8, 126.0, 127.3, 127.4, 127.7, 127.9, 128.0, 128.1, 128.5, 129.0, 130.7, 130.8, 131.0, 134.9, 138.7, 138.9, 139.3, 140.1, 140.2, 140.3, 144.2, 146.2, 157.7, 159.6 ppm; HRMS calculated for $C_{41}H_{34}N_3$ [M$^+$ + H] 568.2753, found: 568.2744.

Synthesis of 2-(piperidin-1-yl)-4,9,11-triphenyl-benzo[*a*]acridine-1-carbonitrile (11)

2-(Piperidin-1-yl)-4,9,11-triphenyl-5,6-dihydrobenzo[*a*]acridine-1-carbonitrile (**10**, 567 mg, 1 mmol) was treated with DDQ (554 mg, 2 mmol) in refluxing benzene for 60 min. After completion, the reaction mixture was filtered and dried over Na_2SO_4 and the solvent was removed *in vacuo*. The crude product obtained was purified by column chromatography on neutral alumina using 10% ethyl acetate in *n*-hexane as the eluent to afford 396 mg (70%) of **11** as a yellow solid: $R_f = 0.78$ (ethyl acetate–*n*-hexane, 1 : 9, v/v); mp (ethyl acetate–*n*-hexane) > 250 °C; MS (ESI) 566 [M + H$^+$]; IR (KBr) $\nu = 2926$ (s), 2855 (m), 2207 (s), 1590 (m) cm^{-1}; ^{1}H NMR (300 MHz, $CDCl_3$): $\delta = 1.66$–1.78 (m, 2H), 1.80–1.96 (m, 4H), 3.40–3.52 (m, 4H), 6.98 (s, 1H), 7.35–7.64 (m, 11H), 7.70–8.01 (m, 6H), 8.19–8.22 (m, 1H), 8.36–8.42 (m, 1H), 10.71 (s, 1H); ^{13}C NMR (75 MHz, $CDCl_3$): $\delta = 24.1$, 26.3, 54.2, 99.4, 120.4, 121.1, 125.8, 126.1, 127.4, 127.5, 127.9, 128.0, 128.3, 128.6, 128.9, 129.1, 129.8, 131.1, 131.5, 133.4, 134.9, 138.5, 139.3, 140.0, 140.2, 140.3, 145.7, 146.3, 147.0, 149.3, 157.7, 159.2 ppm; HRMS calculated for $C_{41}H_{32}N_3$ [M$^+$ + H] 566.2596, found 566.2561.

Conclusions

In summary, we have developed a new efficient methodology for the synthesis of novel bipolar benzo[*f*]quinolines and benzo[*a*] acridines from easily accessible ketene-*S*,*S*-acetal in good yields. We demonstrated that the donor–acceptor partially hydrogenated benzo[*f*]quinolines exhibited non-aggregating behaviour and intense solvatochromism due to intramolecular charge transfer (ICT). We showed that the emission color can be effectively controlled from blue to green to yellow to red by modulating the aromatic π-characteristics not only in solution (photoluminescence) but also in solid electroluminescent devices. Among the four fabricated blue–green–yellow–red devices, the blue organic light emitting device using partially hydrogenated benzo[*f*]quinoline **6c** as an emissive layer showed good *I–L–V* characteristics and stability. An efficient blue flat-panel display was successfully fabricated using dihydrobenzo[*f*]quinoline **6c**, which opens a new avenue for the usage of these nonplanar compounds as emissive materials for further research and development in organic electronics.

Acknowledgements

We gratefully acknowledge financial support from the Department of Science and Technology (DST Ramanna Fellowship to AG & project sanctioned vide DST no. SR/S2/CMP-0050/2008), New Delhi, India. VK and SPS are thankful to UGC and CSIR, New Delhi for research fellowships. The CDRI communication number for the manuscript is 8255. Spectroscopic data provided by SAIF, CDRI is acknowledged.

Notes and references

1 M. Y. Berezin and S. Achilefu, *Chem. Rev.*, 2010, **110**, 2641–2684.
2 (*a*) Z. Xu, J. Yoon and D. R. Spring, *Chem. Soc. Rev.*, 2010, **39**, 1996–2006; (*b*) K. Huang, H. Yang, Z. Zhou, M. Yu, F. Li, X. Gao, T. Yi and C. Huang, *Org. Lett.*, 2008, **10**, 2557–2560.
3 (*a*) B. N. G. Giepmans, S. R. Adams, M. H. Ellisman and R. Y. Tsien, *Science*, 2006, **312**, 217–224; (*b*) M. S. T. Gonçalves, *Chem. Rev.*, 2009, **109**, 190–212.
4 (*a*) H. Klauk, *Chem. Soc. Rev.*, 2010, **39**, 2643–2666; (*b*) C. D. Dimitrakopoulos and D. J. Mascaro, *IBM J. Res. Dev.*, 2001, **45**, 11–27.
5 (*a*) X. Zhang, J. W. Shim, S. P. Tiwari, Q. Zhang, J. E. Norton, P.-T. Wu, S. Barlow, S. A. Jenekhe, B. Kippelen, J.-L. Brédas and S. R. Marder, *J. Mater. Chem.*, 2011, **21**, 4971–4982; (*b*) J.-L. Brédas, J. E. Norton, J. Cornil and V. Coropceanu, *Acc. Chem. Res.*, 2009, **42**, 1691–1699; (*c*) J. J. M. Hall and R. H. Friend, Organic Photovoltaic Devices, in *Clean Electricity from Photovoltaics*, ed. M. D. Archer, Imperial College Press, London, 2001, pp. 377–445.
6 (*a*) T. M. Figueira-Duarte and K. Müllen, *Chem. Rev.*, 2011, **111**, 7260–7314; (*b*) J. Roncali, *Acc. Chem. Res.*, 2000, **33**, 147–156; (*c*) F. J. M. Hoeben, P. Jonkheijm, E. W. Meijer and A. P. H. J. Schenning, *Chem. Rev.*, 2005, **105**, 1491–1546; (*d*) P. F. H. Schwab, J. R. Smith and J. Michl, *Chem. Rev.*, 2005, **105**, 1197–1279; (*e*) S. R. Forrest and M. E. Thompson, *Chem. Rev.*, 2007, **107**, 923–1386; (*f*) K. Komatsu, *Bull. Chem. Soc. Jpn.*, 2007, **80**, 2285–2302; (*g*) A. C. Grimsdale, K. L. Chan, R. E. Martin, P. G. Jokisz and A. B. Holmes, *Chem. Rev.*, 2009, **109**, 897–1091; (*h*) A. L. Kanibolotsky, I. F. Perepichka and P. J. Skabara, *Chem. Soc. Rev.*, 2010, **39**, 2695–2728.
7 (*a*) C. H. Chen and J. M. Shi, *Coord. Chem. Rev.*, 1998, **171**, 161–174; (*b*) Y. Z. Wang and A. J. Epstein, *Acc. Chem. Res.*, 1999, **32**, 217–224; (*c*) M. C. Suh, B. Jiang and T. D. Tilley, *Angew. Chem., Int. Ed.*, 2000, **39**, 2870–2873.
8 C. W. Tang and S. A. VanSlyke, *Appl. Phys. Lett.*, 1987, **51**, 913–915.
9 (*a*) C. J. Tonzola, A. P. Kulkarni, A. P. Gifford, W. Kaminsky and S. A. Jenekhe, *Adv. Funct. Mater.*, 2007, **17**, 863–874; (*b*) A. P. Kulkarni, Y. Zhu, A. Babel, P.-T. Wu and S. A. Jenekhe, *Chem. Mater.*, 2008, **20**, 4212–4223; (*c*) A. Kimyonok, X.-Y. Wang and M. J. Weck, *Polym. Rev.*, 2006, **46**, 47–77.
10 (*a*) X. Zhang, A. S. Shetty and S. A. Jenekhe, *Macromolecules*, 1999, **32**, 7422–7429; (*b*) Y. Zhu, M. M. Alam and S. A. Jenekhe, *Macromolecules*, 2003, **36**, 8958; (*c*) C. J. Tonzola, M. M. Alam, B. A. Bean and S. A. Jenekhe, *Macromolecules*, 2004, **37**, 3554; (*d*) T. W. Kwon, M. M. Alam and S. A. Jenekhe, *Chem. Mater.*, 2004, **16**, 4657.
11 (*a*) L. Duan, J. Qiao, Y. Sun and Y. Qiu, *Adv. Mater.*, 2011, **23**, 1137–1144; (*b*) C. Yang, *Tetrahedron Lett.*, 2010, **51**, 2007–2009.
12 (*a*) A. Goel, S. Chaurasia, M. Dixit, V. Kumar, S. Prakash, B. Jena, J. K. Verma, M. Jain, R. S. Anand and S. S. Manoharan, *Org. Lett.*, 2009, **11**, 1289–1292; (*b*) A. Goel, M. Dixit, S. Chaurasia, A. Kumar, R. Raghunandan, P. R. Maulik and R. S. Anand, *Org. Lett.*, 2008, **10**, 2553–2556; (*c*) R. S. Anand, and S. S. Manoharan, PCT WO/2009/122445, 2009.
13 A. Goel, V. Kumar, S. Chaurasia, M. Rawat, R. Prasad and R. S. Anand, *J. Org. Chem.*, 2010, **75**, 3656–3662.
14 A. Goel, V. Kumar, P. Nag, V. Bajpai, B. Kumar, C. Singh, S. Prakash and R. S. Anand, *J. Org. Chem.*, 2011, **76**, 7474–7481.
15 (*a*) G. Jones, in *Comprehensive Heterocyclic Chemistry II*, ed. A. R. Katritzky, C. W. Rees and E. F. V. Scriven, Pergamon Press, Oxford, 1996, vol. 5, ch. 5.05, pp. 167–243; (*b*) A. R. Katritzky and S. Rachwal, *Chem. Rev.*, 2011, **111**, 7063–7120; (*c*) S. Madapa, V. Singh and S. Batra, *Tetrahedron*, 2006, **62**, 8740–8748.
16 (*a*) S. Majumder, K. R. Gipson and A. L. Odom, *Org. Lett.*, 2009, **11**, 4720–4723; (*b*) X.-S. Wang, Q. Li, C.-S. Yao and S.-J. Tu, *Eur. J. Org. Chem.*, 2008, 3513–3518.
17 A. Goel, S. P. Singh, A. Kumar, R. Kant and P. R. Maulik, *Org. Lett.*, 2009, **11**, 5122–5125.
18 (*a*) Y. Tominaga, *Trends Heterocycl. Chem.*, 1991, **2**, 43–83; (*b*) H. Junjappa, H. Ila and C. V. Asokan, *Tetrahedron*, 1990, **46**, 5423–5506; (*c*) R. K. Dieter, *Tetrahedron*, 1986, **42**, 3029–3096.
19 Y. Huang and R. W. Hartmann, *Synth. Commun.*, 1998, **28**, 1197–1200.
20 G.-W. Wang, C.-S. Jia and Y.-W. Dong, *Tetrahedron Lett.*, 2006, **47**, 1059–1063.
21 N. Miyaura and A. Suzuki, *Chem. Rev.*, 1995, **95**, 2457–2483.
22 N. Mataga, Y. Kaifu and M. Koizumi, *Bull. Chem. Soc. Jpn.*, 1956, **29**, 465–470.